Urban Climate 56 (2024) 102045

Contents lists available at ScienceDirect

Urban Climate

journal homepage: www.elsevier.com/locate/uclim

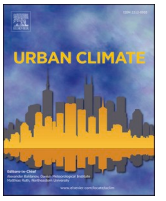

Exploring the non-linear impacts of urban features on land surface temperature using explainable artificial intelligence

Fei Feng [a], Yaxue Ren [b], Chengyang Xu [a], Baoquan Jia [c], Shengbiao Wu [d], Raffaele Lafortezza [b,a,*]

[a] Research Centre of Urban Forestry, Key Laboratory for Silviculture and Forest Ecosystem of State Forestry and Grassland Administration, Beijing Forestry University, Beijing 100083, China
[b] Department of Soil, Plant and Food Sciences, University of Bari Aldo Moro, Via Amendola 165/A 70126, Bari, Italy
[c] Research Institute of Forestry, Chinese Academy of Forestry, Beijing 100091, China
[d] Future Urbanity & Sustainable Environment (FUSE) Lab, Division of Landscape Architecture, Department of Architecture, Faculty of Architecture, The University of Hong Kong, Hong Kong SAR, China

ARTICLE INFO

Keywords:
Shapley additive explanations
Urbanization impact
Land surface temperature
Building structure
Urban vegetation
Urban climate research

ABSTRACT

High land surface temperatures (LST) have emerged as crucial threats to urban ecosystems and sustainable urban development. To better understand and mitigate their impacts, it is essential to analyze the contributing urban features. Against this background, we developed a random forest model enhanced by Explainable Artificial Intelligence (XAI) to analyze the impact features of LST in Beijing, China. By applying the XAI method, our results suggest that the major impact features of LST in Beijing are elevation (44.19%), compactness of impervious surface (17.27%), Normalized Difference Vegetation Index (11.12%), proportion of impervious surface area (8.04%), and tree height (3.83%). Compactness of impervious surface exhibited an overall cooling effect, which became weaker at high values. LST increased with building height, and the trend became weaker as building height reached 5 m. The most important features impacting LST in the inner city are the proportion and height of buildings, whereas in the outer city these features are tree height and the compactness of impervious surfaces. The study applies XAI to explain the non-linear interactions between LST and urban features, offering innovative insights to policy-makers to develop sustainable urban planning strategies. Our findings suggest that increasing green spaces and water bodies as well as controlling building density and height can effectively mitigate heat in dense urban areas and enhance cooling effects.

1. Introduction

The rapid pace of urbanization has given rise to substantial alterations in land surface attributes, thereby disrupting the thermal equilibrium of urban structures and triggering a noticeable escalation in temperatures within urban environments (Kalnay and Cai, 2003; Dadashpoor et al., 2019). As the primary sources of anthropogenic heat and greenhouse gas emissions (Zhou et al., 2023), compact urban environments are associated with high land surface temperature (LST) (Won and Jung, 2023). While many studies have

* Corresponding author at: Department of Soil, Plant and Food Sciences (Di.S.S.P.A.), University of Bari Aldo Moro, Via Amendola 165/A 70126, Bari, Italy.
E-mail address: raffaele.lafortezza@uniba.it (R. Lafortezza).

https://doi.org/10.1016/j.uclim.2024.102045
Received 26 September 2023; Received in revised form 2 June 2024; Accepted 23 June 2024
Available online 28 June 2024

explored the impact of environmental factors on LST (Estoque et al., 2017; Norton et al., 2015), gaps still exist in understanding these complex relationships. This comprehension is crucial for optimizing the urban structure and living environment.

Previous research has primarily focused on the impact that urban features exert on LST, including vegetation cover, water body size, land use, and artificial materials with high heat capacity and conductivity (e.g., concrete and waste heat emissions from different sources) (Chen et al., 2021; Ebrahimi et al., 2022; He et al., 2021). Further studies of urban features impacting LST have been conducted in Asia (Liu et al., 2021; Han et al., 2023; Zhang et al., 2023) Europe (Chen et al., 2022; Schwaab, 2022; Morrison et al., 2023), the Americas (Zhou et al., 2011; Zhang and Sun, 2019) and other global regions (Hamed Fahmy et al., 2023; Karami et al., 2023). A recent review (Kim and Brown, 2021) concludes that the primary factors influencing LST include meteorological elements and urban geometry aspects. These factors affect the urban thermal environment through processes of convection, conduction, and radiation. However, the interactions among these features have been relatively overlooked and are crucial for a comprehensive understanding of urban thermal dynamics.

Numerous models, including linear and non-linear models, have been employed in previous studies investigating LST. As in the studies by Logan et al. (2020) and Lu et al. (2023), linear regression models were used to analyze the relationship between LST and other variables. For example, from the negative correlation between NDVI and LST (Hong et al., 2007), the cooling effect of vegetation can be derived. However, these models often fall short in capturing the complex, non-linear relationships between LST and impact features. Conversely, non-linear models, including machine learning algorithms, have demonstrated a remarkable ability to describe complex relationships(Li et al., 2023). These methods provide enhanced prediction capabilities, but are also prone to “black box” related issues which blur the understanding of their inner workings.

In response to these challenges, recent progress in Explainable Artificial Intelligence (XAI) has significantly facilitated the understanding of underlying physical mechanisms in AI-based models and provided global and fine-scale interpretation abilities of modeling behavior (Fleming et al., 2021; Gevaert, 2022; Gunning et al., 2019; McGovern et al., 2019). XAI introduces novel perspectives for the analysis of impact feature importance ranking and interpreting local effects, demonstrating its effectiveness in interpreting features of AI model (Fu et al., 2023). For instance, (Temenos et al., 2023) developed a convolutional neural network using Shapley additive explanation (SHAP) for land classification of remote sensing data and quantified the contributions of different spectral band values to the classification results. Huang et al. (2023) conducted a comparative analysis of different XAI models and found that SHAP explainable models outperformed other methods like LIME (local interpretable model-agnostic explanations) in predicting soil moisture based on the random forest model.

Nevertheless, a limited number of studies have reported the application of XAI techniques to investigate the relationship between LST and urban features (Kolevatova et al., 2021; Kim et al., 2023). Therefore, this study aimed to develop a machine learning model that employs XAI capability to quantify the contributions of different impact features to LST, using Beijing, China, as the site of analysis. The main objectives of this research are to: i) select the best model (between random forest and multiple linear regression) describing the impacts of urban features on LST; ii) to investigate the distribution of urban features impacting LST; iii) explain the non-linear interactions of each feature with LST and other features using the XAI method; and iv) analyze the contribution of the most important features impacting LST in different thermal contexts.

This interdisciplinary study presents a novel approach for employing the XAI model as state-of-the-art technology to deepen our understanding of the mechanisms underlying the complex relationships between LST and urban features. This innovative methodology not only offers interpretable insights into how various urban elements contribute to LST variations but also underscores the necessity for systematic urban planning to mitigate the urban heat island effect. Applying our approach to Beijing’s diverse urban landscape, this study fills a significant gap in urban climate research and sets a precedent for future studies to employ XAI in environmental science, enhancing both the precision and transparency of complex ecological models.

Table 1
Summary of land surface temperature (LST) and impact feature datasets.

Feature	Source	Spatial resolution	Types	References
LST	Landsat 8	100 m	Environmental	https://developers.google.com/earth-engine/datasets/catalog/LANDSAT_LC08_C02_T1_L2
WAT_P	CLCD	30 m	Environmental	https://zenodo.org/record/5816591
SHR_P	CLCD	30 m	Environmental	https://zenodo.org/record/5816591
GRA_P	CLCD	30 m	Environmental	https://zenodo.org/record/5816591
FOR_P	CLCD	30 m	Environmental	https://zenodo.org/record/5816591
CRO_P	CLCD	30 m	Environmental	https://zenodo.org/record/5816591
BAR_P	CLCD	30 m	Environmental	https://zenodo.org/record/5816591
NDVI	Landsat 8	30 m	Environmental	https://developers.google.com/earth-engine/datasets/catalog/LANDSAT_LC08_C02_T1_L2
TH	GEDI	30 m	Environmental	https://glad.umd.edu/dataset/gedi
DEM	FABDEM	30 m	Environmental	https://data.bris.ac.uk/data/dataset/25wfy0f9ukoge2gs7a5mqpq2j7
As_SoP	FABDEM	30 m	Environmental	Derived from DEM
IMP_P	CLCD	30 m	Anthropogenic	https://zenodo.org/record/5816592
ENN	CLCD	30 m	Anthropogenic	https://zenodo.org/record/5816591
BH	GHS	100 m	Anthropogenic	https://ghsl.jrc.ec.europa.eu/download.php?ds=builtH

WAT_P, proportion of water; SHR_P, proportion of shrub; GRA_P, proportion of grass; FOR_P, proportion of forest; CRO_P, proportion of cropland; BAR_P, proportion of barren; As_SoP, of area facing south on the slope; IMP_P, proportion of impervious; CLCD, China Land Cover Dataset; GEDI, Global Ecosystem Dynamics Investigation; FABDEM, digital elevation model excluding forests and buildings; GHS, Global Human Settlement. (See Fig. 2 for other acronyms of features).

2. Materials and methods

2.1. Study area

As the world's largest developing country, China has experienced dramatic urban expansion since the reform of 1978 (Cai et al., 2020), and its capital city, Beijing, has ranked as one of the fastest growing in China, both economically and in size (Ding and Shi, 2013). Studying LST in Beijing helps to understand how urbanization impacts microclimates, which is crucial for urban planning and sustainable city development. Beijing is located on the northern edge of the North China Plain, with longitudes ranging from 115°25′ to 117°30′E and latitudes ranging from 39°28′ to 41°25′ N, near the Bohai Sea in the east, the Taihang Mountains in the west, and the Yanshan Mountains in the north. The landscape of Beijing is predominantly characterized by mountains and plains. The mountainous area is mainly distributed in the northwest, while the plain area is mostly distributed in the southeast, with an elevation generally 30 to 50 m above sea level. This latter area is also the most densely developed in Beijing, including the built-up areas of the city (Fig. 1).

The climate of Beijing is of the temperate, semi-humid continental monsoon type and features four distinct seasons. The annual temperature is relatively moderate, with an average ranging from 10 °C to 12 °C. The winter is cold and dry, with an average temperature of −4.7 °C in January, whereas the summer is hot and humid, registering an average temperature of 26 °C in July. The average annual precipitation level in Beijing is 626 mm, with approximately 80% concentrated in summer.

2.2. Data

The boundaries of the city of Beijing were extracted using the 30-m global artificial impervious area (GAIA) and global urban boundary (GUB) (http://data.ess.tsinghua.edu.cn/gub.html) data (Fig. 2a). For a comprehensive analysis of LST impact features datasets for 2018 were used, including LST, DEM (digital elevation model), NDVI (Normalized Difference Vegetation Index), LC (land cover), TH (tree height), As_SoP (the proportion of area facing south on slopes) and BH (building height). The LST and NDVI data (Fig. 2b, c, respectively) from June to September in 2018 were derived from the Landsat 8 collection 2 dataset on Google Earth Engine, preprocessed to remove cloud-contaminated pixels and corrected for atmospheric and geometric inconsistencies (Cook, 2014). DEM data (Fig. 2d) were derived from FABDEM (Copernicus digital elevation model, excluding forests and buildings), with buildings and forests removed using a machine learning model (Hawker et al., 2022), and were further used to calculate As_SoP. Land cover data (Fig. 2e) were obtained from the Landsat-based annual China land cover dataset (CLCD) and classified using the random forest model and spatial-temporal filtering method to enhance consistency (Yang and Huang, 2021). The Euclidean nearest-neighbor (ENN) distance data (Fig. 2f) were calculated using the Euclidean proximity index of impervious surfaces based on LC data. TH data (Fig. 2g) were extracted from the global forest height map, which was derived from the combination of the Global Ecosystem Dynamics Investigation (GEDI), a merged product of a regression tree ensemble model incorporating GEDI, LiDAR, and Landsat data, ensuring reliable forest height estimation (Marziliano et al., 2013; Lafortezza and Giannico, 2019; Potapov et al., 2021). BH data (Fig. 2h) were

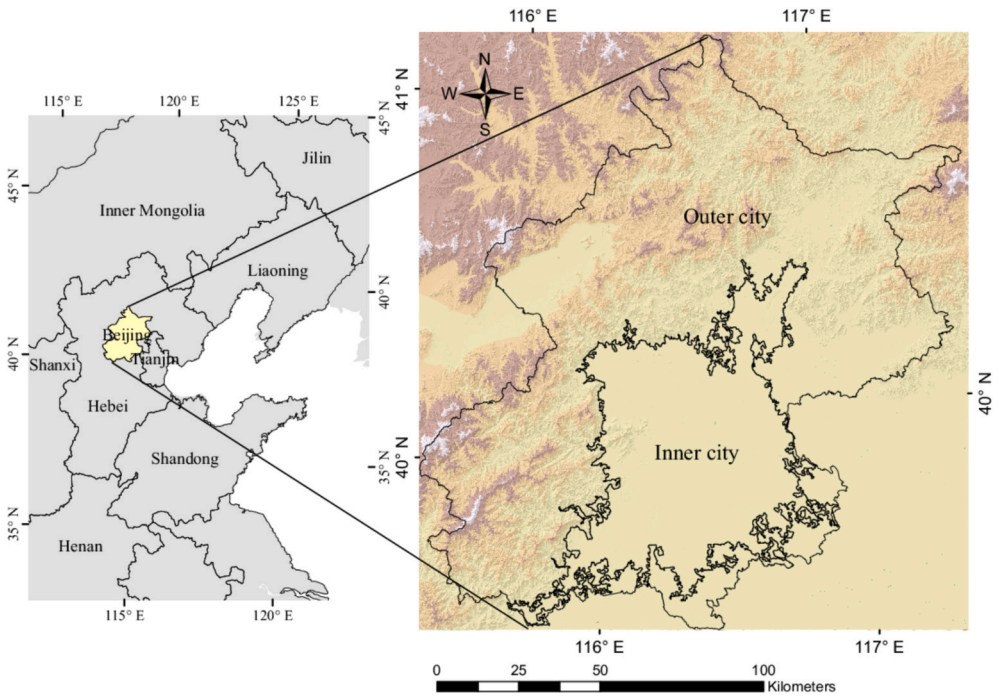

Fig. 1. Location map of the study area. The background map of Beijing (right) is a hillshade image generated from a digital elevation model.

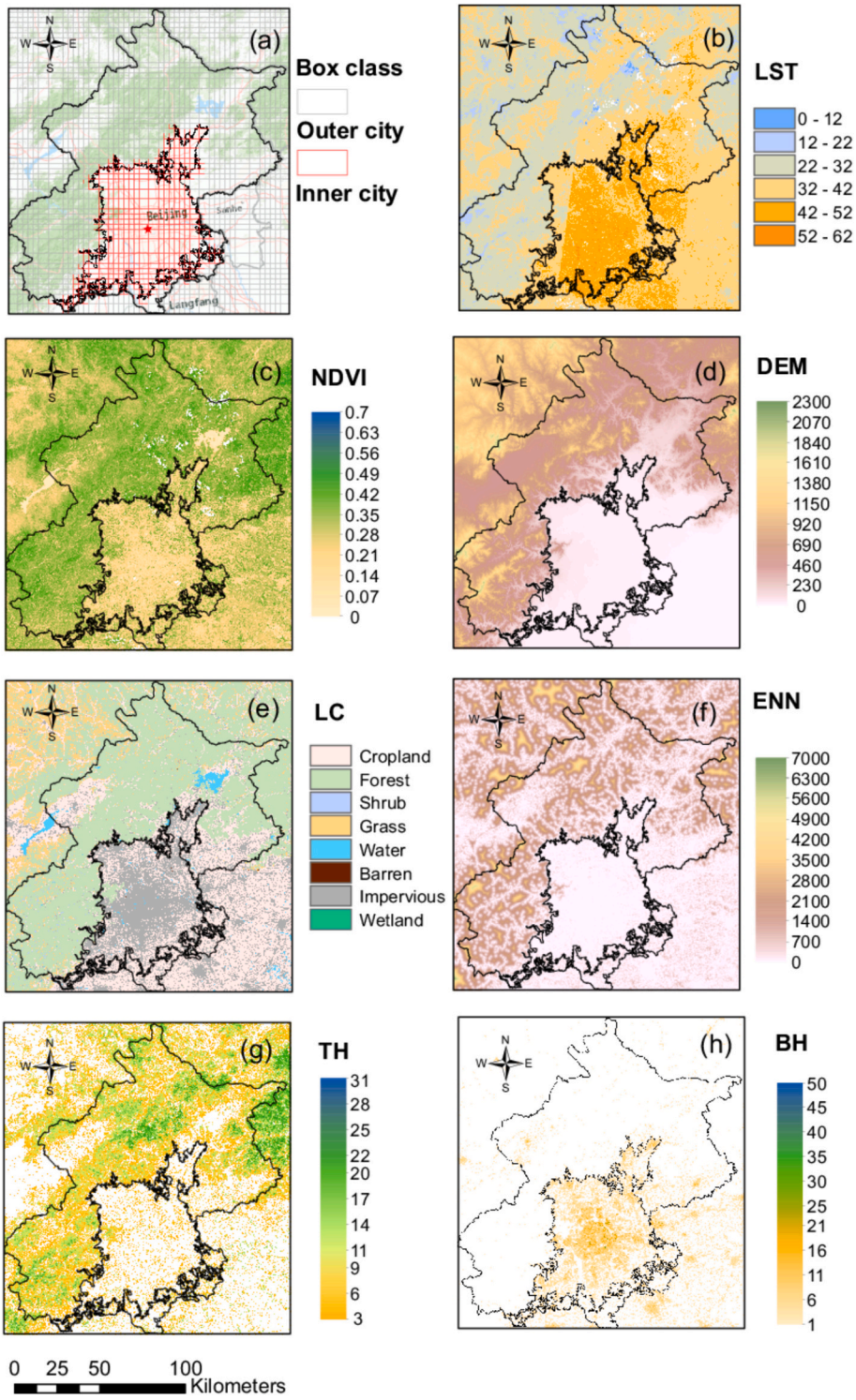

Fig. 2. Spatial distribution of the sample boxes LST, NDVI, DEM, LC, ENN, TH and BH in Beijing, China. (a) Boundary of inner and outer city. (b) LST, land surface temperature (unit: °C); (c) NDVI, Normalized Difference Vegetation Index; (d) DEM, Digital Elevation Model (unit: m); (e) LC, land cover; (f) ENN, Euclidean nearest-neighbor (unit: m); (g) TH, tree height (unit: m); (h) BH, building height (unit: m).

collected from the Global Human Settlement (GHS) dataset, processed through multi-scale convolutional, morphological, and textural transforms by merging ALOS World 3D, Shuttle Radar Topography Mission and Sentinel 2 composite data (Pesaresi et al., 2021), and validated against ground measurements in various cities to analyze 3D urban constructs. To integrate different data sources and conduct spatial analysis, all datasets were projected and resampled to ensure that they incorporated the same coordinate system and 30-m resolution.

2.3. Methodology

2.3.1. Random forest model

This study aims to quantify the contributions of different impact features to LST in both the inner city and outer city areas of Beijing by applying XAI in constructing a random forest (RF) model (Fig. 3). LST is the dependent variable, reflecting the key indicator of urban heat environment. Independent variables, including NDVI, LC, ENN, DEM, As_SoP, TH, and BH, were chosen due to their associations with regulating urban heat environment.

The main steps of the data analysis include: (1) Data collection and preprocessing: all data were uniformly projected and resampled to 30-m resolution; invalid values were removed. (2) Feature values extraction: A 3 × 3 km grid was created within the study area to extract the average values of influencing factors in each grid cell. (3) Model development: The RF model was used to predict LST and compared with traditional multiple linear regression (MLR) models. (4) Model results: The SHAP method was applied to explain the non-linear impacts of each feature in model predictions (Fig. 3).

Firstly, the 3 × 3 km grid was created using ArcGIS covering all the administrative boundaries of Beijing with individual boxes having a side length of 3 km. For each box the mean values were extracted for LST, NDVI, DEM, LC, ENN, TH, BH, and the proportion of each land use type. A total of 3416 sample boxes were detected in the entire study area, 674 of which were considered as inner city boxes and the remaining as outer city boxes.

Secondly, we built a RF model and a MLR model based on the impact feature data obtained above to compare their performances.

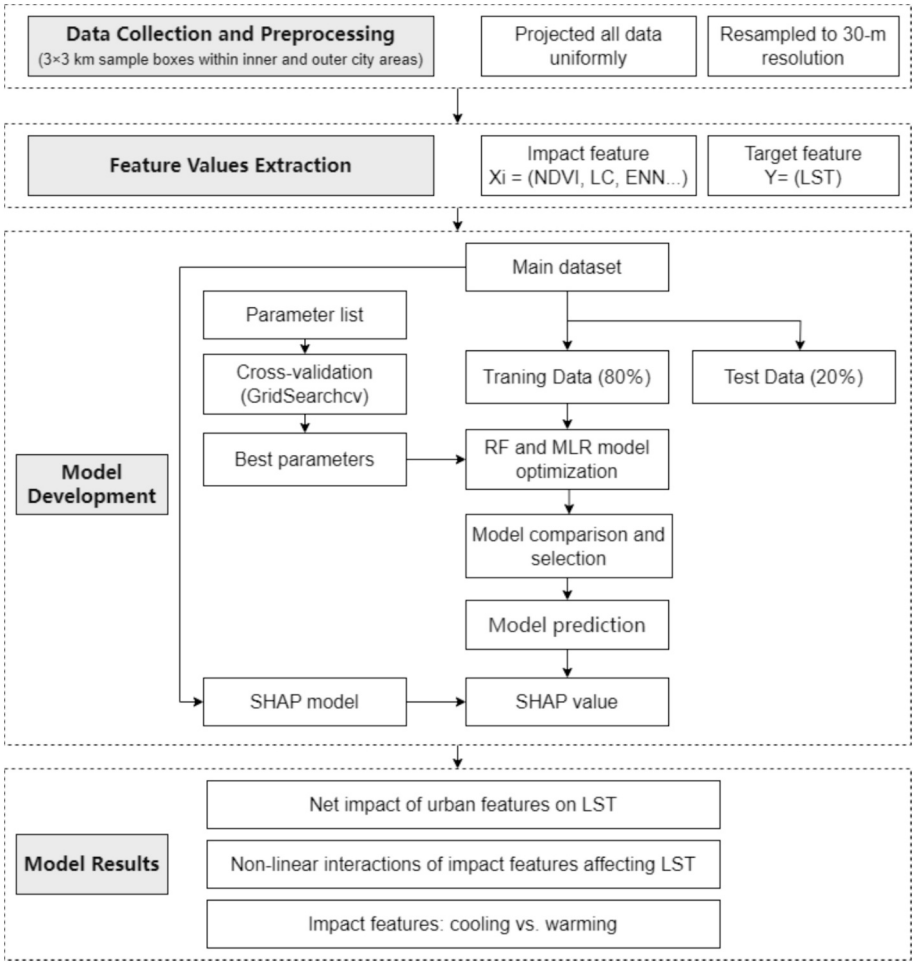

Fig. 3. Flowchart of the data analysis process.

MLR is a classical statistical method used to model the relationship between a dependent variable and multiple independent variables. The RF model was finally selected for its superior performance. Eighty percent of the dataset was employed as the training set, while 20% was randomly selected as validation data. To ensure the stability of the RF model, we conducted 100 cross-validation iterations to make it stable and defined hyperparametric grids for tuning. Specifically, GridSearchCV was used to optimize the maximum number of decision trees and the number of split features (optimized parameters: 500 estimators, max.10 features).

2.3.2. SHAP interpretation for LST prediction

Although the RF model has advantages in processing high-dimensional data, reducing overfitting risks, evaluating feature importance, and parallel computing, its interpretability is far inferior to traditional MLR models, which are subject to AI black box problems of machine learning (McGovern et al., 2019). Therefore, the SHAP method was applied to solve this issue and visualize the non-linear impact between LST and impact features. The basic theory of SHAP, referred to as the Shapely value method proposed by Shapley (1952), has been employed in the field of cooperative games with the aim to solve conflicts. The Shapley value is calculated based on the marginal contribution of the members to the alliance, which has the advantage that the benefits shared by the members are equal to the average of the marginal benefits they create for their participating alliance. The specific formula is as follows:

$$\delta_i(v) = \sum_{K \epsilon N} \frac{[(|K|-1)!(n-|K|)!]}{n!} \times [v(K) - v(K(i))]$$

$$Zi = Z_b + h(x_{i1}) + h(x_{i2}) \ldots + h(x_{ij})$$

In a cooperative game system, the variable n represents the total number of players, and N is the set of members (1, 2, …, n). K is a subset of N that consists of different players. The benefits of the alliance S are represented by $v(K)$, while $\delta_i(v)$ indicates the benefits obtained by player i in the alliance K. The number of players in the alliance K is denoted by $|K|$. $n!$ signifies the factorial of n. $S(i)$ represents the set obtained after removing player i from K. The marginal contribution of member i participating in different alliances, K, is expressed as $[v(K) - v(K(i))]$. The weight of the benefits created by member i in the entire alliance is denoted as $[(|K|-1)!(n-|K|)!]n!$. Zi represents the predicted value of the i-th sample. Z_b refers to the RF model's baseline, and $h(xij)$ represents the contribution of the j-th feature of the i-th sample to the final prediction of LST.

The SHAP value is an additional feature attribution method that interprets the predicted values of the model as the sum of attribution values for each input feature. Therefore, the positive or negative SHAP values (x_{ij}) express the specific impact of different features in the study area in the prediction of LST.

3. Results

3.1. Comparison between the random forest and multiple linear regression model

The relationship between LST and impact features was not a simple linear one, as can be seen in Fig. 4. In the scatter plot, the x-axis represents the observed LST values, and the y-axis represents the LST predicted by the models. The high R^2 value of the RF model (0.89 vs 0.83) indicates that it could more precisely explain the relationship between LST and impact features. The RF model exhibited smaller RMSE (2.10 vs 2.65) and negative biases (−0.035 vs −0.056), indicating that it could predict LST more accurately. Taken together, the RF model was generally superior to the MLR model. Therefore, it was used in this study to capture the complexity of non-linear relationships between LST and impact features given the ability to outperform other models.

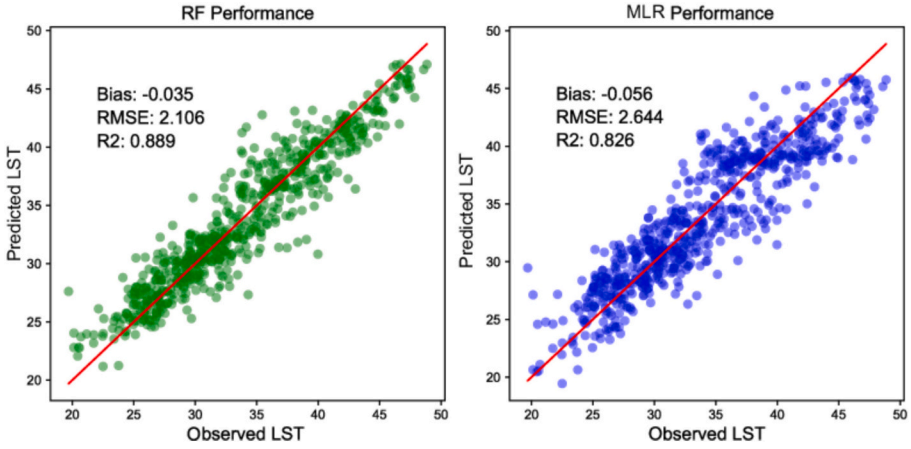

Fig. 4. Validation of the random forest (RF) model and multiple model linear regression (MLR). LST, land surface temperature; R^2, coefficient of determination; RMSE, root mean square error.

3.2. Distribution of urban features impacting LST in the study area

As shown in Fig. 5, the features affecting LST were arranged according to importance in descending order from top to bottom. The y-axis shows the different impact features and the x-axis displays each sample's SHAP value, with red indicating a positive impact (warming) and blue a negative impact (cooling). For each feature, sample points were stacked vertically; the greater the height of the y-axis, the more samples were distributed. We calculated and visualized the SHAP values of the features for all boxes (Fig. 5a), inner city (Fig. 5b), and outer city (Fig. 5c) boxes to analyze their impact on LST by comparing and sorting the absolute SHAP values (Table 2). Overall, the mean value of DEM (DEM_MEAN, 44.19%), ENN (ENN_MEAN, 17.27%), NDVI (NDVI_MEAN, 11.12%), the proportion of IMP (IMP_P, 8.04%), and the mean value of TH (TH_MEAN, 3.83%) were the most important features affecting LST (Fig. 5a). Undoubtedly, the LST changes were mainly impacted by the local landscape and closely related to the compactness of urban buildings. The impact of IMP_P and BH_MEAN on LST was greater in inner cities (Fig. 5b) compared to all boxes (Fig. 5a), while the impact of TH_MEAN on LST was greater in outer cities (Fig. 5c).

3.3. Non-linear interactions of impact features with LST and other features

3.3.1. Interactions of IMP_P, ENN, and BH with LST and other features

Anthropogenic features, including IMP_P, ENN_MEAN, and BH_MEAN, were selected to analyze their interactions with LST and other features across all sample boxes (Fig. 6). These impact features were closely related to the composition and configuration of the urban landscape. IMP_P generally showed a warming effect on LST, and as IMP_P increased the warming effect also increased in an almost linear pattern. In addition, we observed interactions between IMP_P and environmental features that influence LST, including NDVI_MEAN, TH_MEAN, FOR_P, and WAT_P. Specifically, when IMP_P was low and the impacts of these environmental features were large, then the warming effect of IMP_P was mitigated (Fig. 6b-e). This suggests that the presence of vegetation, forests, and water bodies can counteract the heat-retaining capacity of impervious surfaces, consistent with findings from other studies (Beaumont et al., 2022; Norton et al., 2015). As IMP_P increased, BH_MEAN also increased (Fig. 6d); this led to a stronger warming effect on LST.

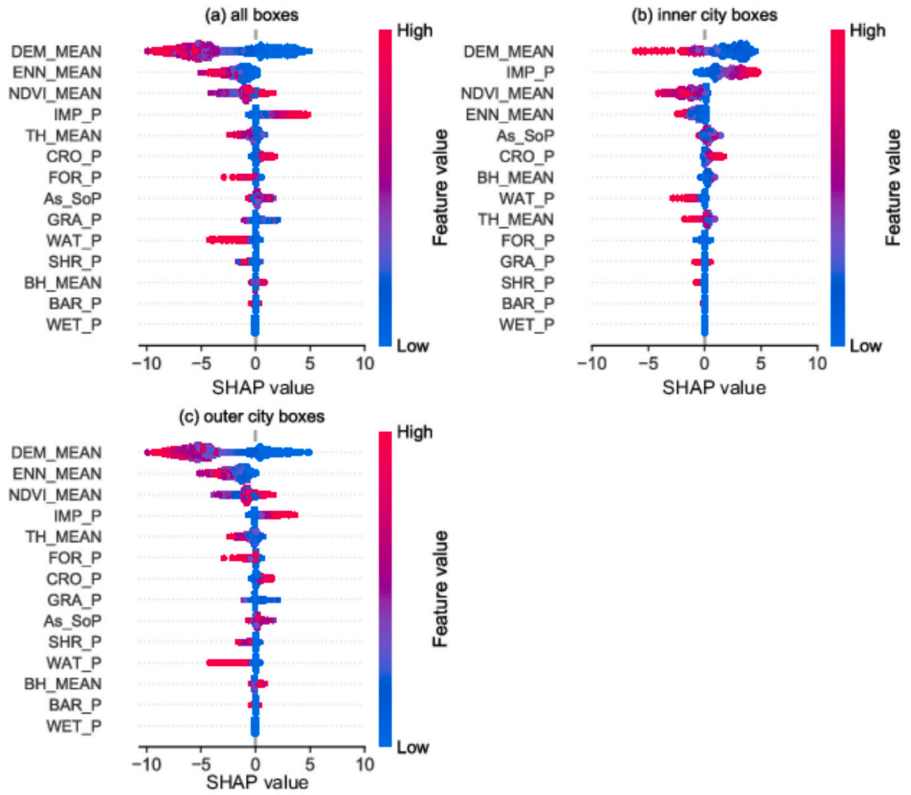

Fig. 5. Contribution of features of the random forest model for (a) all boxes, (b) inner city boxes and (c) outer city boxes. The SHAP value expresses the specific impact of different features on land surface temperature. DEM, digital elevation model; ENN, Euclidean nearest-neighbor; NDVI, Normalized Difference Vegetation Index; TH, tree height; BH, building height; IMP, impervious surface area; CRO, cropland area; FOR, forest area; As_SoP, proportion of area facing south on the slope; GRA, grassland area; WAT, water bodies; SHR, shrubland; BAR, barren land; and WET, wetland.

Table 2
The net impact of urban features on land surface temperature.

Features	All boxes	Inner city boxes	Outer city boxes
DEM_MEAN	44.19	29.76	47.30
ENN_MEAN	17.27	8.90	19.07
NDVI_MEAN	11.12	14.75	10.33
IMP_P	8.04	26.44	4.07
TH_MEAN	3.83	2.85	4.04
BH_MEAN	1.38	3.34	0.95
CRO_P	3.19	4.27	2.95
FOR_P	3.06	1.55	3.38
As_SoP	2.61	4.86	2.13
GRA_P	1.99	0.30	2.36
WAT_P	1.90	2.86	1.69
SHR_P	1.41	0.09	1.70
BAR_P	0.02	0.02	0.02
WET_P	0.00	0.00	0.00

* The net impact of each feature is determined by its average SHAP value.
** For acronym definitions the reader is referred to Fig. 2.

ENN_MEAN, a measure of the spatial compactness of impervious surfaces, generally showed a negative (cooling) effect on LST. When the ENN_MEAN increased, environmental features such as NDVI_MEAN and TH_MEAN increased as well and the cooling effect became stronger (Fig. 6g, h), indicating a synergistic relationship between urban greenery and surface cooling. Similar results were also found in the study by Zhao et al. (Zhao et al., 2020). As ENN_MEAN gradually increased, the cooling effect rate of ENN_MEAN gradually slowed down.

BH_MEAN, categorized as an urban structural feature, showed the opposite warming patterns on LST. When BH_MEAN was low, the warming effect rate rapidly increased as BH_MEAN increased. However, when the BH_MEAN was high (e.g., exceeded 5 m), the warming effect rate weakened and maintained a relatively high SHAP value ranging from 0.25 to 0.75 (Fig. 6l-o). This previous study also noted a plateau in the warming effect of BH on LST beyond a certain threshold (Wang and Xu, 2021). It is also worth noting the boundaries with SHAP values of 0. For example, in Fig. 4 (m), SHAP values are negative in areas with low BH_MEAN and high TH_MEAN. This suggests that the driving effect on LST values is negative in these areas, implying that low building height and high tree height contribute to mitigating UHI effect.

3.3.2. Interactions of IMP_P, ENN, and BH with LST and other features across all samples, inner city and outer city samples

We further analyzed the interaction between different features across all samples, inner city samples, and outer city samples. For anthropogenic features, shown in Fig. 7, when IMP_P increased, NDVI_MEAN showed a gradually decreasing trend (Fig. 7a0-a2). This suggests that a higher IMP_P might have a negative impact on green space cover and vegetation growth, which are essential for temperature regulation through evapotranspiration and shading effects (Obiakor et al., 2012). In both the inner city and outer city samples, the interaction pattern between IMP_P and NDVI_MEAN appeared to be similar.

ENN_MEAN, which reflects the spatial distribution of impervious surfaces, influenced the urban cooling effect in a non-linear manner. For ENN_MEAN, as compactness increased, the cooling effect increased as well, but as compactness further increased (>400 m for inner city boxes, >2000 m for other boxes), the increase of the cooling effect tended to flatten out. As ENN_MEAN increased, NDVI_MEAN showed a gradually increasing trend. It is also worth noting that in the inner city samples (Fig. 7c1), ENN_MEAN was mainly concentrated in the range of <200 m, indicating that the layout of buildings in inner city areas was relatively compact.

3.4. Contribution of the most important features impacting LST in different thermal contexts

To compare and specifically explore the relationship between LST and impact features in different thermal contexts, fishnet box samples with LST of the 1st and 99th percentiles in the entire study area and 1st and 99th percentiles in the inner city area were counted and analyzed as four case studies, respectively. For the entire study area, Fig. 8a displays the features (i.e., IMP_P, DEM, and As_SoP) contributing the most positive effects (warming) to LST in hot samples (LST of the 99th percentile). Correspondingly, Fig. 8b illustrates the features (i.e., DEM_MEAN, ENN_MEAN, TH_MEAN, and FOR_P) contributing the most negative effects (cooling) to LST in cold samples (LST of the 1st percentile). These findings suggest that elevation (DEM), the proportion (IMP_P) and compactness (ENN) of impervious surface area exerted a significant impact on LST from all data, including both cold and hot samples. The case studies of inner cities showed similar results. Notably, compared with the result of the entire study area where TH and FOR_P contributed to the cooling effect on LST (Fig. 8b), Fig. 8d shows that NDVI and WAT_P played a role in impacting the LST of inner cities.

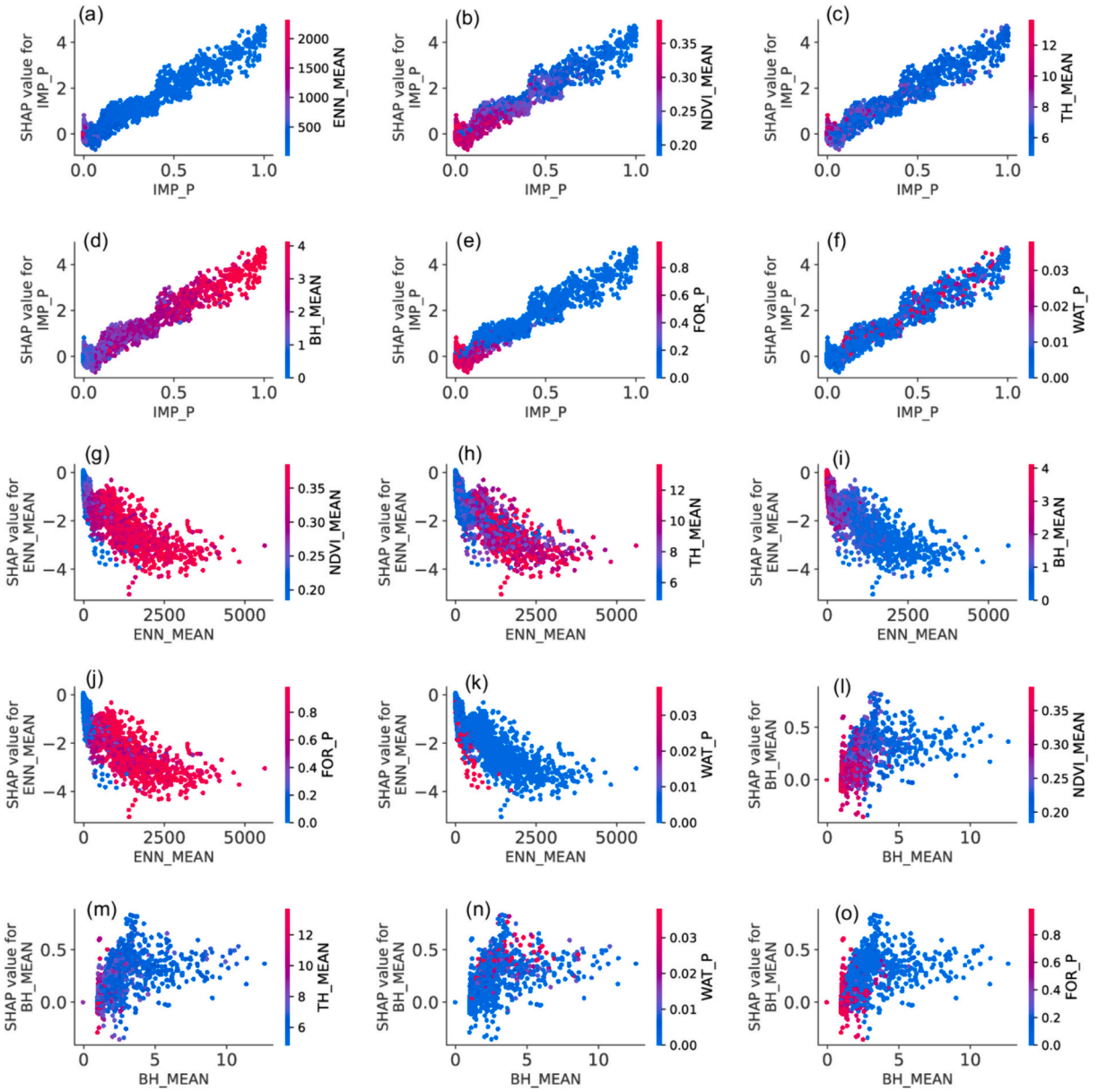

Fig. 6. Dependence plot for interactions of IMP_P, ENN, and BH with land surface temperature and other features. The SHAP value expresses the specific impact of different features. The colour of the dots from red to blue represent the value of the features, as shown by the bars on the right. (See Fig. 2 and Table 1 for acronym definitions). (For interpretation of the references to colour in this figure legend, the reader is referred to the web version of this article.)

4. Discussion

4.1. Advantages of the XAI machine learning model

Linear regression models have been commonly applied to investigate the relationship between LST and its impact features (Aghazadeh et al., 2023; Zhang et al., 2021; D. Zhou et al., 2022a). For example, five patch-level landscape metrics of green cover classes showed a significant relationship with LST based on the stepwise linear regression model (Asgarian et al., 2015). However, we found that the RF model outperformed the MLR model in predicting LST, demonstrating complex non-linear relationships between LST and impact features (Section 3.1). Although Wang et al. (2023) found that urban landscape components are strong explainers of LST in Beijing using linear spatial autocorrelation analysis, our results are consistent with those of Oukawa et al. (2022). These authors also compared the MLR model with the RF model and showed that MLR is only able to explain a modest percentage of variance in urban

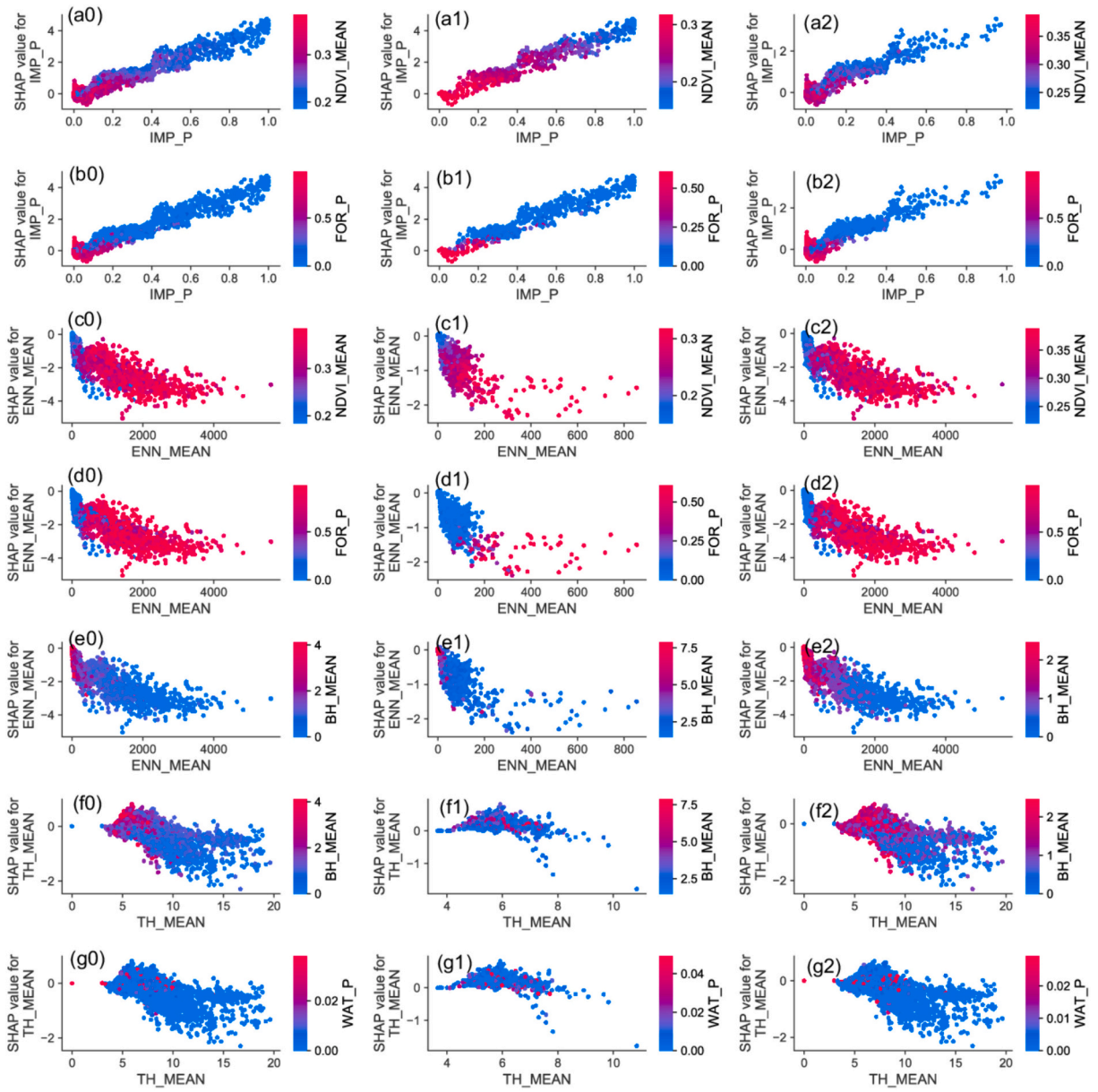

Fig. 7. Dependence plot for interactions of IMP_P, ENN, and BH with land surface temperature and other features across all samples, inner city samples, and outer city samples. The SHAP value expresses the specific impact of different features. The colour of the dots from red to blue represent the value of the features, as shown by the bars on the right. (See Fig. 2 and Table 1 for acronym definitions). (For interpretation of the references to colour in this figure legend, the reader is referred to the web version of this article.)

heat island intensity (64% and 34% for daytime and nighttime, respectively), while the RF model exhibited a superior performance with explanatory power over 96% of the variance for both daytime and nighttime conditions.

Moreover, the XAI machine learning model coupled with the RF model used in this study not only surpasses the traditional linear regression model, but also solves the transparency problem associated with machine learning methods. The XAI method employed in this study assigns a SHAP value to the features of each fishnet box, representing their contribution to LST in the RF model.

4.2. Relationship between LST and impact features

In this study, we explored the relationship between LST and its impact features in the study area of Beijing, China. Previous studies have shown that LST is closely influenced by urban landscape configurations, such as patch size, shape and land use type (Arnfield, 2003; Zhou et al., 2011; Jung et al., 2021). Our results show that DEM_MEAN, ENN_MEAN, NDVI_MEAN, and TH_MEAN were the most

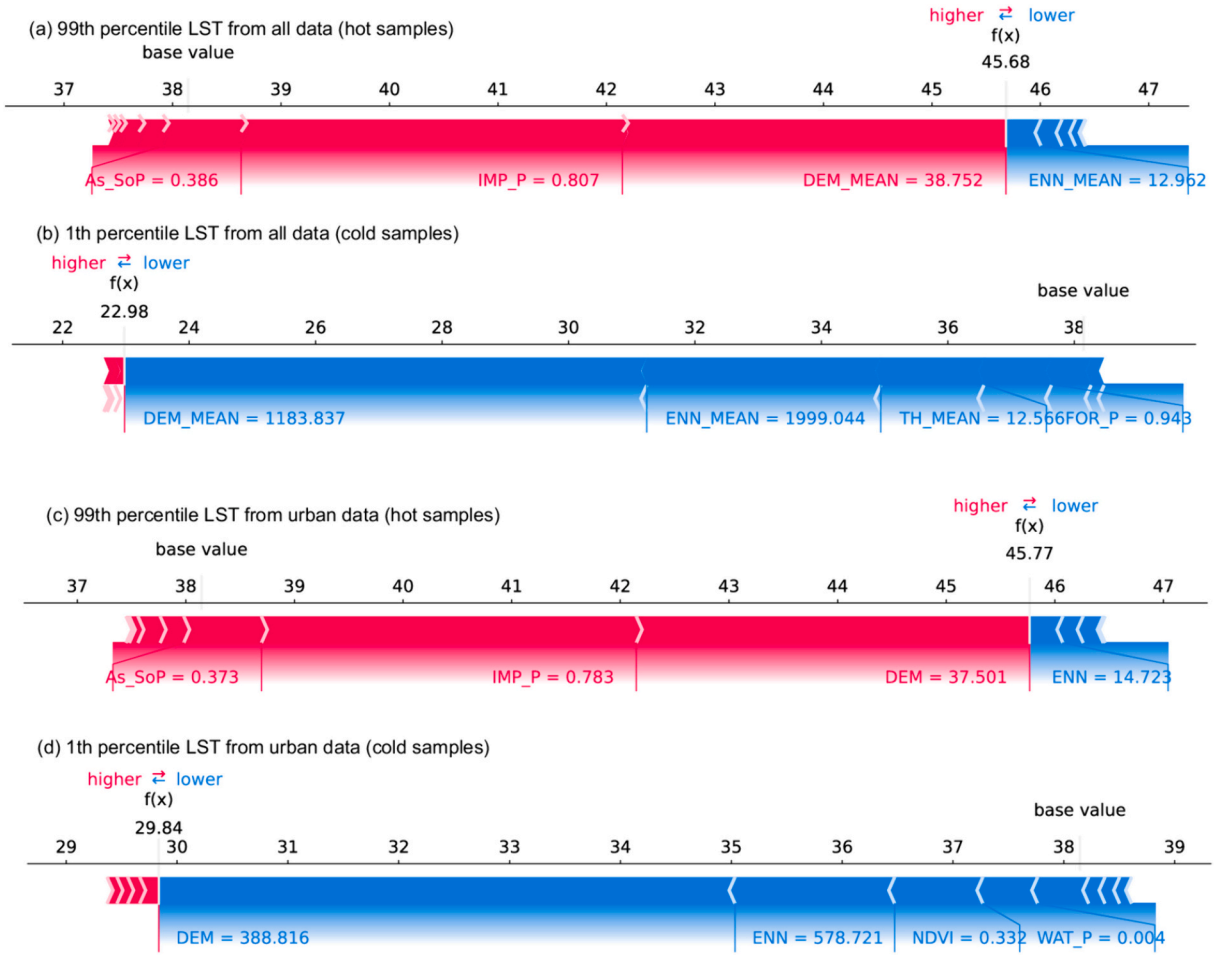

Fig. 8. Force plot of features that contributed the most to impacting LST in four case studies. The subplots (a) and (c) show the hot samples (LST of the 99th percentile) from all data and inner city data. The subplots (b) and (d) show the cold samples (LST of the 1st percentile) from all data and inner city data. The red bars represent the warming effect and blue bars the cooling effect. The length of the bar indicates impact intensity. (For interpretation of the references to colour in this figure legend, the reader is referred to the web version of this article.)

important features regulating LST in Beijing. An increase in DEM_MEAN had the greatest impact on the LST of the entire region and displayed a stronger cooling trend. The IMP_P and BH_MEAN contributed the most to increasing LST, while the ENN, NDVI and WAT_P were key features in reducing LST in urban areas. For all samples, including inner and outer cities, TH_MEAN and FOR_P were effective in decreasing LST. The study findings suggest that increasing green spaces and water bodies while reducing the compactness of buildings and properly controlling building density and height could effectively decrease temperatures in urban areas.

Our results are consistent with those of previous studies demonstrating that water and vegetation contribute negatively to LST, whereas built-up areas contribute positively to LST (Zhang and Sun, 2019; Liu et al., 2021; Bala et al., 2021; Chen et al., 2022). Furthermore, we quantified the interactive effects and intensity of positive and negative contributions of these features. The interaction of features impacting LST revealed an inverse relationship between IMP_P and vegetation characteristics (TH, FOR_P), with a linear trend impact of IMP_P on LST. In comparison with previous studies that provide general patterns of landscape configurations (Sanesi et al., 2007; Zhang and Sun, 2019; L. Zhou et al., 2022b), our research more thoroughly demonstrates the non-linear interactions of impact features with LST and other features. For example, urban areas with low ENN were more likely to exhibit low TH and a weak cooling effect. Contrarily, urban areas with high ENN generally showed low BH and elevated TH with a strong cooling effect. The case studies further revealed that ENN plays a crucial role in regulating LST in both hot and cold samples.

4.3. Study implications and policy recommendations

Our study highlights the important cooling effect of environmental features such as vegetation and water bodies on LST. Therefore, urban planning policies should prioritize the preservation and expansion of existing green and blue spaces. With regard to anthropogenic features, our study reveals that building height positively correlates with LST, especially up to a height of 5 m, which suggests that tall buildings can provide shading effects in densely built areas. Consequently, it behooves policy-makers to promote the design of

buildings that facilitate air circulation and reduce heat retention. By integrating these recommendations into urban planning and policy-making, cities can become more sustainable and thermally resilient environments.

4.4. Uncertainties and limitations

Uncertainties may arise from analyzing LST using satellite data. Considering the close relationship between solar radiation and daytime temperatures, Huang et al. (2016) reported that the sampling error within a 5 × 5-km^2 region was 1.4% for solar radiation in monthly time scales, which suggests that uncertainties could be smaller for the LST results derived from the 3 × 3-km box used in this study. We also noticed that the feature data collected might contain uncertainties due to factors such as instrumentation, processing methods, misclassification and calibration (Schiavina et al., 2022; Yang and Huang, 2021). In this study we applied a SHAP method (based on fishnet boxes) to account for these potential uncertainties.

Variance inflation factor (VIF) is a standard metric for assessing multicollinearity in linear models. We calculated VIF values for each impact feature (Appendix A, Table), However, tree-based models like the RF model have low sensitivity to multicollinearity. The random sampling of features at each node creation helps reduce the effect of multicollinearity (Kurniati et al., 2023). All impact features were used due to the ability of the random forest model to effectively manage multicollinearity. Furthermore, we used the SHAP model by employing the Tree Explainer, and SHAP values do not assume feature independence (Aas et al., 2021).

Despite the presence of limitations, this study provides insight into the complex relationship between LST and various impact features. Future research endeavors could further investigate additional features that may contribute to variations in LST. In general, the findings from this research can help inform efforts to mitigate hot urban environments (e.g., urban heat islands).

5. Conclusions

The utilization of Explainable Artificial Intelligence (XAI) coupled with the RF model in this study provides a profound leap in understanding the non-linear relationships that govern LST. This capability not only surpasses that of traditional linear regression models but also addresses the transparency issues typically associated with machine learning methodologies, making our study results more interpretable and actionable. Our detailed analysis highlights the relevance of the compactness of impervious surfaces in mitigating urban LST, with decreasing compactness leading to a greater cooling effect when the Euclidean nearest-neighbor distance for impervious surface areas ranges from 0 to 2000 m. These findings can equip policy-makers and urban planners with the data needed to implement strategies that effectively reduce LST, such as optimizing green space distribution and adjusting urban layout, ultimately contributing to the creation of thermally comfortable urban environments.

This study provides a more comprehensive understanding of how urban planning elements can modulate temperature. The complex non-linear interactions between LST and urban impact features emphasize the need for mitigating hot urban environments by designing new green space and water bodies while reducing impervious surfaces. From a practical standpoint, this work offers valuable insights and guidance to urban planners and policy-makers in their quest to build more sustainable and livable urban environments.

Authorship contribution statement

Fei Feng and **Raffaele Lafortezza:** Designed the study, collected the data, performed the analysis and drafted the original manuscript and its revision. **Yaxue Ren,** drafted the original manuscript and its revision. **Chengyang Xu, Baoquan Jia** and **Shengbiao Chen** contributed to discussions on the scientific issue and to the revision.

CRediT authorship contribution statement

Fei Feng: Writing – review & editing, Writing – original draft, Validation, Formal analysis, Data curation, Conceptualization. **Yaxue Ren:** Writing – review & editing, Writing – original draft, Data curation. **Chengyang Xu:** Resources, Project administration, Data curation. **Baoquan Jia:** Investigation. **Shengbiao Wu:** Investigation, Data curation. **Raffaele Lafortezza:** Writing – review & editing, Writing – original draft, Supervision, Methodology, Investigation, Funding acquisition, Data curation, Conceptualization.

Declaration of competing interest

The authors declare that they have no known competing financial interests or personal relationships that could have appeared to influence the work reported in this paper.

Data availability

Data will be made available on request.

Acknowledgments

This study was funded by the Fundamental Research Funds for the Central Universities (BLX 202201) and carried out under the research project “CLEARING HOUSE - Collaborative Learning in Research, Information-sharing and Governance on How Urban tree-

based solutions support Sino-European urban futures", funded by the European Union's Horizon 2020 Research and Innovation Program (Grant Agreement No. 821242). We would like to thank Yole DeBellis for revising the manuscript.

Appendix A. Supplementary data

Supplementary data to this article can be found online at https://doi.org/10.1016/j.uclim.2024.102045.

References

Aas, K., Jullum, M., Løland, A., 2021. Explaining individual predictions when features are dependent: more accurate approximations to Shapley values. Artif. Intell. 298, 103502 https://doi.org/10.1016/j.artint.2021.103502.

Aghazadeh, F., Bageri, S., Garajeh, M.K., Ghasemi, M., Mahmodi, S., Khodadadi, E., Feizizadeh, B., 2023. Spatial-temporal analysis of day-night time SUHI and its relationship between urban land use, NDVI, and air pollutants in Tehran metropolis. Appl. Geomat. 15, 697–718. https://doi.org/10.1007/s12518-023-00515-w.

Arnfield, A.J., 2003. Two decades of urban climate research: a review of turbulence, exchanges of energy and water, and the urban heat island. Int. J. Climatol. 23, 1–26. https://doi.org/10.1002/joc.859.

Asgarian, A., Amiri, B.J., Sakieh, Y., 2015. Assessing the effect of green cover spatial patterns on urban land surface temperature using landscape metrics approach. Urban Ecosyst. 18, 209–222. https://doi.org/10.1007/s11252-014-0387-7.

Bala, R., Prasad, R., Yadav, V.P., 2021. Quantification of urban heat intensity with land use/land cover changes using Landsat satellite data over urban landscapes. Theor. Appl. Climatol. 145, 1–12. https://doi.org/10.1007/s00704-021-03610-3.

Beaumont, B., Loozen, Y., Castin, T., Radoux, J., Wyard, C., Lauwaet, D., Lefebre, F., Halford, T., Haid, M., Defourny, P., Hallot, E., 2022. Green infrastructure planning through eo and gis analysis: the canopy plan of liège, Belgium, to mitigate its urban heat island. In: ISPRS Annals of the Photogrammetry, Remote Sensing and Spatial Information Sciences, pp. 243–250. https://doi.org/10.5194/isprs-Annals-V-4-2022-243-2022.

Cai, Z., Liu, Q., Cao, S., 2020. Real estate supports rapid development of China's urbanization. Land Use Policy 95, 104582. https://doi.org/10.1016/j.landusepol.2020.104582.

Chen, J., Zhan, W., Jin, S., Han, W., Du, P., Xia, J., Lai, J., Li, J., Liu, Z., Li, L., Huang, F., Ding, H., 2021. Separate and combined impacts of building and tree on urban thermal environment from two- and three-dimensional perspectives. Build. Environ. 194, 107650 https://doi.org/10.1016/j.buildenv.2021.107650.

Chen, S., Haase, D., Qureshi, S., Firozjaei, M.K., 2022. Integrated land use and urban function impacts on land surface temperature: implications on urban heat mitigation in Berlin with eight-type spaces. Sustain. Cities Soc. 83, 103944 https://doi.org/10.1016/j.scs.2022.103944.

Cook, M., 2014. Atmospheric Compensation for a Landsat Land Surface Temperature Product. Theses.

Dadashpoor, H., Azizi, P., Moghadasi, M., 2019. Land use change, urbanization, and change in landscape pattern in a metropolitan area. Sci. Total Environ. 655, 707–719. https://doi.org/10.1016/j.scitotenv.2018.11.267.

Ding, H., Shi, W., 2013. Land-use/land-cover change and its influence on surface temperature: a case study in Beijing City. Int. J. Remote Sens. 34, 5503–5517. https://doi.org/10.1080/01431161.2013.792966.

Ebrahimi, A., Motamedvaziri, B., Nazemosadat, S.M.J., Ahmadi, H., 2022. Investigating the land surface temperature reaction to the land cover patterns during three decades using landsat data. Int. J. Environ. Sci. Technol. 19, 159–172. https://doi.org/10.1007/s13762-021-03294-2.

Estoque, R.C., Murayama, Y., Myint, S.W., 2017. Effects of landscape composition and pattern on land surface temperature: an urban heat island study in the megacities of Southeast Asia. Sci. Total Environ. 577, 349–359. https://doi.org/10.1016/j.scitotenv.2016.10.195.

Fleming, S.W., Watson, J.R., Ellenson, A., Cannon, A.J., Vesselinov, V.C., 2021. Machine learning in earth and environmental science requires education and research policy reforms. Nat. Geosci. 14, 878–880. https://doi.org/10.1038/s41561-021-00865-3.

Fu, C., Huang, Z., Scheuer, B., Lin, J., Zhang, Y., 2023. Integration of dockless bike-sharing and metro: prediction and explanation at origin-destination level. Sustain. Cities Soc. 99, 104906 https://doi.org/10.1016/j.scs.2023.104906.

Gevaert, C.M., 2022. Explainable AI for earth observation: a review including societal and regulatory perspectives. Int. J. Appl. Earth Obs. Geoinf. 112, 102869 https://doi.org/10.1016/j.jag.2022.102869.

Gunning, D., Stefik, M., Choi, J., Miller, T., Stumpf, S., Yang, G.-Z., 2019. XAI-Explainable artificial intelligence. Sci. Robot. 4 https://doi.org/10.1126/scirobotics.aay7120 eaay7120.

Hamed Fahmy, A., Amin Abdelfatah, M., El-Fiky, G., 2023. Investigating land use land cover changes and their effects on land surface temperature and urban heat islands in Sharqiyah Governorate, Egypt. Egypt. J. Remote Sens. Space Sci. 26, 293–306. https://doi.org/10.1016/j.ejrs.2023.04.001.

Han, L., Lu, L., Fu, P., Ren, C., Cai, M., Li, Q., 2023. Exploring the seasonality of surface urban heat islands using enhanced land surface temperature in a semi-arid city. Urban Clim. 49, 101455 https://doi.org/10.1016/j.uclim.2023.101455.

Hawker, L., Uhe, P., Paulo, L., Sosa, J., Savage, J., Sampson, C., Neal, J., 2022. A 30 m global map of elevation with forests and buildings removed. Environ. Res. Lett. 17, 024016 https://doi.org/10.1088/1748-9326/ac4d4f.

He, W., Cao, S., Du, M., Hu, D., Mo, Y., Liu, M., Zhao, J., Cao, Y., 2021. How do two- and three-dimensional urban structures impact seasonal land surface temperatures at various spatial scales? A case study for the northern part of Brooklyn, New York, USA. Remote Sens. 13, 3283. https://doi.org/10.3390/rs13163283.

Hong, S., Lakshmi, V., Small, E.E., 2007. Relationship between vegetation biophysical properties and surface temperature using multisensor satellite data. J. Clim. 20, 5593–5606. https://doi.org/10.1175/2007JCLI1294.1.

Huang, G., Li, X., Huang, C., Liu, S., Ma, Y., Chen, H., 2016. Representativeness errors of point-scale ground-based solar radiation measurements in the validation of remote sensing products. Remote Sens. Environ. 181, 198–206. https://doi.org/10.1016/j.rse.2016.04.001.

Huang, F., Zhang, Yongkun, Zhang, Ye, Nourani, V., Li, Q., Li, L., Shangguan, W., 2023. Towards interpreting machine learning models for predicting soil moisture droughts. Environ. Res. Lett. 18, 074002 https://doi.org/10.1088/1748-9326/acdbe0.

Jung, M.C., Dyson, K., Alberti, M., 2021. Urban landscape heterogeneity influences the relationship between tree canopy and land surface temperature. Urban For. Urban Green. 57, 126930 https://doi.org/10.1016/j.ufug.2020.126930.

Kalnay, E., Cai, M., 2003. Impact of urbanization and land-use change on climate. Nature 423, 528–531. https://doi.org/10.1038/nature01675.

Karami, P., Tavakoli, S., Esmaeili, M., 2023. Monitoring spatiotemporal impacts of changes in land surface temperature on near eastern fire salamander (Salamandra infraimmaculata) in the Middle East. Heliyon 9, e17241. https://doi.org/10.1016/j.heliyon.2023.e17241.

Kim, S.W., Brown, R.D., 2021. Urban heat island (UHI) intensity and magnitude estimations: a systematic literature review. Sci. Total Environ. 779, 146389 https://doi.org/10.1016/j.scitotenv.2021.146389.

Kim, M., Kim, D., Jin, D., Kim, G., 2023. Application of explainable artificial intelligence (XAI) in urban growth modeling: a case study of Seoul Metropolitan Area, Korea. Land 12, 420. https://doi.org/10.3390/land12020420.

Kolevatova, A., Riegler, M.A., Cherubini, F., Hu, X., Hammer, H.L., 2021. Unraveling the impact of land cover changes on climate using machine learning and explainable artificial intelligence. Big Data Cogn. Comput. 5, 55. https://doi.org/10.3390/bdcc5040055.

Kurniati, B., Dewi, Y., Hadi, A., 2023. Handling multicollinearity on social spatial data using geographically weighted random Forest. SAR J. - Sci. Res. 149–153. https://doi.org/10.18421/SAR63-02.

Lafortezza, R., Giannico, V., 2019. Combining high-resolution images and LiDAR data to model ecosystem services perception in compact urban systems. Ecol. Indic. 96, 87–98. https://doi.org/10.1016/j.ecolind.2017.05.014.
Li, F., Yigitcanlar, T., Nepal, M., Nguyen, K., Dur, F., 2023. Machine learning and remote sensing integration for leveraging urban sustainability: a review and framework. Sustain. Cities Soc. 96, 104653 https://doi.org/10.1016/j.scs.2023.104653.
Liu, F., Hou, H., Murayama, Y., 2021. Spatial interconnections of land surface temperatures with land cover/use: a case study of Tokyo. Remote Sens. 13, 610. https://doi.org/10.3390/rs13040610.
Logan, T.M., Zaitchik, B., Guikema, S., Nisbet, A., 2020. Night and day: the influence and relative importance of urban characteristics on remotely sensed land surface temperature. Remote Sens. Environ. 247, 111861 https://doi.org/10.1016/j.rse.2020.111861.
Lu, L., Fu, P., Dewan, A., Li, Q., 2023. Contrasting determinants of land surface temperature in three megacities: implications to cool tropical metropolitan regions. Sustain. Cities Soc. 92, 104505 https://doi.org/10.1016/j.scs.2023.104505.
Marziliano, P.A., Lafortezza, R., Colangelo, G., Davies, C., Sanesi, G., 2013. Structural diversity and height growth models in urban forest plantations: a case-study in northern Italy. Urban Forest. Urban Green. 12 (2), 246–254. https://doi.org/10.1016/j.ufug.2013.01.006.
McGovern, A., Lagerquist, R., John Gagne, D., Jergensen, G.E., Elmore, K.L., Homeyer, C.R., Smith, T., 2019. Making the black box more transparent: understanding the physical implications of machine learning. Bull. Am. Meteorol. Soc. 2175–2199. https://doi.org/10.1175/BAMS-D-18-0195.1.
Morrison, W., Grimmond, S., Kotthaus, S., 2023. Simulating satellite urban land surface temperatures: sensitivity to sensor view angle and assumed landscape complexity. Remote Sens. Environ. 293, 113579 https://doi.org/10.1016/j.rse.2023.113579.
Norton, B.A., Coutts, A.M., Livesley, S.J., Harris, R.J., Hunter, A.M., Williams, N.S.G., 2015. Planning for cooler cities: a framework to prioritise green infrastructure to mitigate high temperatures in urban landscapes. Landsc. Urban Plan. 134, 127–138. https://doi.org/10.1016/j.landurbplan.2014.10.018.
Obiakor, M.O., Ezeonyejiaku, C.D., Mogbo, T.C., 2012. Effects of vegetated and synthetic (impervious) surfaces on the microclimate of urban area. J. Appl. Sci. Environ. Manag. 16, 85–94.
Oukawa, G.Y., Krecl, P., Targino, A.C., 2022. Fine-scale modeling of the urban heat island: a comparison of multiple linear regression and random forest approaches. Sci. Total Environ. 815 https://doi.org/10.1016/j.scitotenv.2021.152836.
Pesaresi, M., Corbane, C., Ren, C., Edward, N., 2021. Generalized vertical components of built-up areas from global digital elevation models by multi-scale linear regression modelling. PLoS One 16, e0244478. https://doi.org/10.1371/journal.pone.0244478.
Potapov, P., Li, X., Hernandez-Serna, A., Tyukavina, A., Hansen, M.C., Kommareddy, A., Pickens, A., Turubanova, S., Tang, H., Silva, C.E., Armston, J., Dubayah, R., Blair, J.B., Hofton, M., 2021. Mapping global forest canopy height through integration of GEDI and Landsat data. Remote Sens. Environ. 253, 112165 https://doi.org/10.1016/j.rse.2020.112165.
Sanesi, G., Lafortezza, R., Marziliano, P.A., Ragazzi, A., Mariani, L., 2007. Assessing the current status of urban forest resources in the context of Parco Nord, Milan, Italy. Landsc. Ecol. Eng. 3 (2), 187–198. https://doi.org/10.1007/s11355-007-0031-2.
Schiavina, M., Melchiorri, M., Pesaresi, M., Panagiotis, P., Freire, S., Maffenini, L., Goch, K., Tommasi, P., Kemper, T., 2022. GHSL Data Package 2022. https://doi.org/10.2760/19817.
Schwaab, J., 2022. Sprawl or compactness? How urban form influences urban surface temperatures in Europe. City Environ. Interact. 16, 100091 https://doi.org/10.1016/j.cacint.2022.100091.
Shapley, L.S., 1952. A Value for N-Person Games. RAND Corporation.
Temenos, A., Temenos, N., Kaselimi, M., Doulamis, A., Doulamis, N., 2023. Interpretable deep learning framework for land use and land cover classification in remote sensing using SHAP. IEEE Geosci. Remote Sens. Lett. 20, 1–5. https://doi.org/10.1109/LGRS.2023.3251652.
Wang, M., Xu, H., 2021. The impact of building height on urban thermal environment in summer: a case study of Chinese megacities. PLoS One 16, e0247786. https://doi.org/10.1371/journal.pone.0247786.
Wang, X., Zhang, Y., Yu, D., 2023. Exploring the relationships between land surface temperature and its influencing factors using multisource spatial big data: a case study in Beijing, China. Remote Sens. 15, 1783. https://doi.org/10.3390/rs15071783.
Won, J., Jung, M.C., 2023. Does compact development mitigate urban thermal environments? Influences of smart growth principles on land surface temperatures in Los Angeles and Portland. Sustain. Cities Soc. 90, 104385 https://doi.org/10.1016/j.scs.2022.104385.
Yang, J., Huang, X., 2021. The 30 m annual land cover dataset and its dynamics in China from 1990 to 2019. Earth Syst. Sci. Data 13, 3907–3925. https://doi.org/10.5194/essd-13-3907-2021.
Zhang, Y., Sun, L., 2019. Spatial-temporal impacts of urban land use land cover on land surface temperature: case studies of two Canadian urban areas. Int. J. Appl. Earth Obs. Geoinf. 75, 171–181. https://doi.org/10.1016/j.jag.2018.10.005.
Zhang, Q., Wu, Z., Singh, V., Liu, C., 2021. Impacts of spatial configuration of land surface features on land surface temperature across urban agglomerations, China. Remote Sens. 13, 4008. https://doi.org/10.3390/rs13194008.
Zhang, Z., Luan, W., Yang, J., Guo, A., Su, M., Tian, C., 2023. The influences of 2D/3D urban morphology on land surface temperature at the block scale in Chinese megacities. Urban Clim. 49, 101553 https://doi.org/10.1016/j.uclim.2023.101553.
Zhao, J., Zhao, X., Liang, S., Zhou, T., Du, X., Xu, P., Wu, D., 2020. Assessing the thermal contributions of urban land cover types. Landsc. Urban Plan. 204, 103927 https://doi.org/10.1016/j.landurbplan.2020.103927.
Zhou, W., Huang, G., Cadenasso, M.L., 2011. Does spatial configuration matter? Understanding the effects of land cover pattern on land surface temperature in urban landscapes. Landsc. Urban Plan. 102, 54–63. https://doi.org/10.1016/j.landurbplan.2011.03.009.
Zhou, D., Xiao, J., Frolking, S., Zhang, L., Zhou, G., 2022a. Urbanization contributes little to global warming but substantially intensifies local and regional land surface warming. Earths. Future 10. https://doi.org/10.1029/2021EF002401 e2021EF002401.
Zhou, L., Yuan, B., Hu, F., Wei, C., Dang, X., Sun, D., 2022b. Understanding the effects of 2D/3D urban morphology on land surface temperature based on local climate zones. Build. Environ. 208 https://doi.org/10.1016/j.buildenv.2021.108578.
Zhou, X., Huang, Z., Scheuer, B., Wang, H., Zhou, G., Liu, Y., 2023. High-resolution estimation of building energy consumption at the city level. Energy 275, 127476. https://doi.org/10.1016/j.energy.2023.127476.